ELSEVIER

Comput. Methods Appl. Mech. Engrg. 191 (2001) 717–726

Computer methods in applied mechanics and engineering

www.elsevier.com/locate/cma

Fluid–structure interactions of a parachute crossing the far wake of an aircraft

T. Tezduyar *, Y. Osawa [1]

*Team for Advanced Flow Simulation and Modeling (T*AFSM), Mechanical Engineering and Materials Science, Rice University – MS 321, 6100 Main Street, Houston, TX 77005, USA*

Received 25 September 2000; received in revised form 19 January 2001

Abstract

In this paper we describe a computational technique for simulation of the fluid–structure interactions of a parachute crossing the far wake of an aircraft. This technique relies on using the long-wake flow data already computed, in our case, with the Multi-Domain Method (MDM) we developed earlier. The fluid–structure interaction computations are carried out over a domain enclosing the parachute and moving with the payload. This domain functions as one of the subdomains of the MDM designed specifically for the parachute fluid–structure interactions considered here. The boundary conditions for this subdomain are extracted from the long-wake flow data, at locations corresponding to the positions of those boundaries in the subdomain over which the wake flow data were computed. The Navier–Stokes equations of incompressible flows, governing the fluid dynamics, are solved with the Deforming-Spatial-Domain/Stabilized Space–Time (DSD/SST) formulation, which can handle changes in the spatial domain occupied by the fluid. This formulation is coupled to the finite element formulation used for solving the membrane equations governing the structural mechanics of the parachute canopy and the equations governing the mechanics of the suspension lines. The numerical example included demonstrates how the technique described here, functioning as a component of the MDM, enables us to simulate the fluid–structure interactions of a parachute crossing an aircraft wake.

1. Introduction

In a multi-aircraft paratrooper deployment, as a parachute deployed from an aircraft crosses during its descent the wake of the preceding aircraft, it might become subjected to strong, unsteady aerodynamic forces. Although normally the distance between the two aircraft is quite large compared to the length scales of the aircraft, it may not be large enough for the parachute to be spared from these wake effects. Fluid–structure interactions play a significant role in the aerodynamic and structural response of the parachute to the wake effects, and need to be accounted for in numerical prediction of the parachute behavior.

In addition to the formidable task involved in solving an unsteady fluid–structure interaction problem, the need to accurately solve unsteady flows over long-wake regions poses a substantial challenge. This challenge motivated us to develop the Multi-Domain Method (MDM) [1] for the class of simulations requiring computation of the long-wake flows generated by a primary object and, sometimes, the influence of this wake on a secondary object placed far downstream. In the MDM, the problem domain is divided into a sequence of overlapping subdomains. The primary object is placed in the first subdomain, and the subsequent subdomains cover the long-wake regions and secondary objects. While the inflow boundary

* Corresponding author. Tel.: +1-713-527-6051; fax: +1-713-285-5423.
E-mail address: tezduyar@rice.edu; http://www.mems.rice.edu/TAFSM/ (T. Tezduyar).
[1] Present address: Tire Research Department, Bridgestone Corporation, 3-1-1 Ogawahigashi-cho, Kodaira-shi, Tokyo 187, Japan.

0045-7825/01/$ - see front matter
PII: S0045-7825(01)00311-5

conditions for the first subdomain are derived from the free-stream conditions, the inflow conditions for each of the remaining subdomains are extracted from the subdomain preceding it.

In 3D applications of the MDM reported in [2–4], we tested this method by computing the flow around a small wing placed in the wake of a larger wing; computation of the first and second phases of the Karman vortex street in the wake of a circular cylinder up to 300 diameters downstream; and preliminary computation of the aerodynamics of a rigid parachute crossing the wake of an aircraft. A more comprehensive study of a rigid parachute crossing an aircraft wake, together with the MDM developed for this purpose, was presented in [5].

In this paper we describe the computational technique developed for simulation of the fluid–structure interactions of the parachute. This technique functions rather independently from the computation of the long-wake flow data that it relies on using. The wake data may have been computed earlier for a different purpose, or may have just been computed based specifically on the conditions of the parachute problem we wish to simulate. In the extreme case, the wake data can be computed almost concurrently with the computation of the parachute problem, provided that the wake computation is at least one time step ahead of the parachute computation.

The parachute fluid–structure interactions are computed over a domain that moves with the payload and traverses the space also covered by the domain used for computation of the wake flow. Therefore the parachute domain functions as one of the subdomains of the MDM designed specifically for simulating the parachute fluid–structure interactions considered here. The boundary conditions for the parachute domain are extracted from the flow field computed over the wake domain, at locations corresponding to the positions of those boundaries in the wake domain.

The fluid dynamics part of the problem is governed by the Navier–Stokes equations of incompressible flows. The structural dynamics part is governed by the nonlinear membrane equations, taking into account large displacements and rotations, but assuming small strains, as well as the equations governing the mechanics of the parachute suspension lines.

The Navier–Stokes equations are solved with the Deforming-Spatial-Domain/Stabilized Space–Time (DSD/SST) formulation [6–8]. The DSD/SST formulation was developed as a general-purpose method for computation of flows with moving boundaries and interfaces, such as two-fluid flows and fluid–structure interactions. This method automatically takes into account the motion of the boundaries and interfaces. At each time step of a computation, the locations of the boundaries and interfaces are calculated as part of the overall solution. The stabilized space–time formulations were used earlier by other researchers to solve problems with fixed spatial domains (see for example [9]). The DSD/SST formulation is based on the Galerkin/Least-Squares (GLS) formulation [10,11]. The Streamline-Upwind/Petrov–Galerkin (SUPG) [12,13] and Pressure-Stabilizing/Petrov–Galerkin (PSPG) [6] formulations are the essential components of the GLS formulation. When these stabilized formulations are implemented with a sound understanding of their underlying concepts, flows at high Reynolds numbers can be computed without introducing excessive numerical dissipation, and equal-order interpolation functions for velocity and pressure can be used to simplify the implementation.

Another component of the DSD/SST formulation is an automatic mesh moving technique, which is used for updating the mesh as the spatial domain occupied by the fluid changes its shape every time step. This mesh moving method, first introduced in [14], is based on moving the nodal points as governed by the equations of linear elasticity. The motion of the internal nodes is determined by solving these additional equations, with the boundary conditions for these mesh motion equations specified in such a way that they match the normal velocity of the fluid at the fluid–structure interface. For additional details, see [14].

The DSD/SST formulation is coupled to the finite element formulation used for solving the membrane equations governing the structural mechanics of the parachute canopy and the equations governing the mechanics of the suspension lines. These coupled formulations have recently been applied also to simulation of the fluid–structure interactions for a round parachute descending through a wake-free (or uniform) environment (see [15]) and for a gliding ram-air parachute (see [16]). Here they are used in a computational technique that serves as a component of the MDM that has been designed for simulation of the fluid–structure interactions of a parachute crossing an aircraft wake.

Discretization of the fluid–structure interaction problem addressed here results in large, coupled nonlinear equation systems that need to be solved at every time step. The coupling between the blocks of

equations corresponding to the Navier–Stokes, mesh moving, and membrane equations is handled in an iterative fashion. At each nonlinear iteration, the vectors of unknowns associated with these three blocks of equations are updated individually, based on the Newton–Raphson method. While updating the vector of unknowns associated with one of the blocks, we use the most recently updated values of the vectors of unknowns associated with the other two blocks. The coupled, linear equation system that needs to be solved in updating each of the three vectors of unknowns is also solved iteratively, with the GMRES search technique [17]. We have implemented these solution techniques for distributed-memory parallel computing, and the results reported here were obtained by carrying out the computations on a CRAY T3E-1200.

In Section 2, we review the governing equations of fluid and structural mechanics. The DSD/SST formulation is described in Section 3, and the finite element formulation for structural mechanics is described in Section 4. The numerical example is presented in Section 5, and the concluding remarks are provided in Section 6.

2. Governing equations

2.1. Fluid mechanics

Let $\Omega_t \subset \mathbb{R}^{n_{sd}}$ be the spatial fluid mechanics domain with boundary Γ_t at time $t \in (0,T)$, where the subscript t indicates the time-dependence of the spatial domain and its boundary. The Navier–Stokes equations of incompressible flows can be written as:

$$\rho\left(\frac{\partial \mathbf{u}}{\partial t} + \mathbf{u}\cdot\nabla\mathbf{u} - \mathbf{f}\right) - \nabla\cdot\boldsymbol{\sigma} = 0 \quad \text{on } \Omega_t \quad \forall t \in (0,T), \tag{1}$$

$$\nabla\cdot\mathbf{u} = 0 \quad \text{on } \Omega_t \quad \forall t \in (0,T), \tag{2}$$

where ρ, $\mathbf{u}$ and $\mathbf{f}$ are the density, velocity and the external force, respectively. The stress tensor $\boldsymbol{\sigma}$ is defined as

$$\boldsymbol{\sigma}(p,\mathbf{u}) = -p\mathbf{I} + 2\mu\boldsymbol{\varepsilon}(\mathbf{u}). \tag{3}$$

Here p, $\mathbf{I}$ and μ are the pressure, identity tensor and the viscosity, respectively. The strain rate tensor $\boldsymbol{\varepsilon}(\mathbf{u})$ is defined as

$$\boldsymbol{\varepsilon}(\mathbf{u}) = \frac{1}{2}\left((\nabla\mathbf{u}) + (\nabla\mathbf{u})^{\mathrm{T}}\right). \tag{4}$$

Both Dirichlet- and Neumann-type boundary conditions are accounted for:

$$\begin{aligned} &\mathbf{u} = \mathbf{g} \quad \text{on } (\Gamma_t)_g, \\ &\mathbf{n}\cdot\boldsymbol{\sigma} = \mathbf{h} \quad \text{on } (\Gamma_t)_h. \end{aligned} \tag{5}$$

Here $(\Gamma_t)_g$ and $(\Gamma_t)_h$ are the complementary subsets of the boundary Γ_t, $\mathbf{n}$ is the unit normal vector at the boundary, and $\mathbf{g}$ and $\mathbf{h}$ are the given functions. A divergence-free velocity field is specified as the initial condition.

2.2. Structural mechanics

Let $\Omega_t^s \subset \mathbb{R}^{n_{sd}}$ be the spatial structural mechanics domain with boundary Γ_t^s at time $t \in (0,T)$, where the superscript s implies structural mechanics, and $n_{sd} = 2$ for membranes and $n_{sd} = 1$ for cables. The governing equations obtained from conservation of linear momentum are written as follows:

$$\rho^s\left(\frac{\mathrm{d}^2\mathbf{y}}{\mathrm{d}t^2} - \mathbf{f}^s\right) - \nabla\cdot\boldsymbol{\sigma}^s = 0 \quad \text{on } \Omega_t^s \quad \forall t \in (0,T). \tag{6}$$

Here ρ^s, $\mathbf{y}$, $\mathbf{f}^s$ and $\boldsymbol{\sigma}^s$ are the material density, displacements, external body forces, and Cauchy stress tensor, respectively. In this study, we assume small strains, and therefore use linear stress–strain relations for the membrane and cable structures. However, the large displacements and rotations involved make this class of problems nonlinear. For the membrane elements, plane stress conditions are assumed, and therefore the constitutive equations are written as follows:

$$S^{ij} = \left\{\overline{\lambda}_m G^{ij} G^{kl} + \mu_m (G^{il} G^{jk} + G^{ik} G^{jl})\right\} E_{kl}, \tag{7}$$

where

$$\overline{\lambda}_m = \frac{2\lambda_m \mu_m}{(\lambda_m + 2\mu_m)}. \tag{8}$$

Here λ_m and μ_m are the Lamé constants, the subscript m denotes the membrane, and G^{ij} are the components of the contravariant metric tensor [18,19]. For the cable elements, uniaxial stress condition is assumed, and therefore the constitutive equation becomes

$$S^{11} = E_c G^{11} G^{11} E_{11}, \tag{9}$$

where E_c is the Young's modulus and the subscript c denotes the cable. Both Dirichlet- and Neumann-type boundary conditions are considered, and are expressed as:

$$\begin{aligned} &\mathbf{y} = \mathbf{g}^s \quad \text{on } (\Gamma_t^s)_g, \\ &\mathbf{n} \cdot \boldsymbol{\sigma}^s = \mathbf{h}^s \quad \text{on } (\Gamma_t^s)_h. \end{aligned} \tag{10}$$

Here $(\Gamma_t^s)_g$ and $(\Gamma_t^s)_h$ are the complementary subsets of the boundary Γ_t^s, $\mathbf{n}$ is the unit normal vector at the boundary, and $\mathbf{g}^s$ and $\mathbf{h}^s$ are the given functions. The initial conditions are specified as

$$\mathbf{y} = \mathbf{0}, \qquad \frac{\mathrm{d}\mathbf{y}}{\mathrm{d}t} = \mathbf{0} \quad \text{on } \Omega_0^s. \tag{11}$$

3. DSD/SST formulation

In discretization of the space–time domain, the time interval $(0, T)$ is partitioned into subintervals $I_n = (t_n, t_{n+1})$, where t_n and t_{n+1} belong to an ordered series of time levels $0 = t_0 < t_1 < \cdots < t_N = T$. Let $\Omega_n = \Omega_{t_n}$ and $\Gamma_n = \Gamma_{t_n}$ to simplify the notation. The space–time slab Q_n is defined as the domain enclosed by the surfaces Ω_n, Ω_{n+1}, and P_n, where P_n is the lateral surface of Q_n described by the boundary Γ_n as t traverses I_n. The Dirichlet- and Neumann-type boundary conditions are specified over $(P_n)_g$ and $(P_n)_h$. For this discretization, the finite element trial function spaces $(\mathcal{S}_{\mathbf{u}}^h)_n$ for velocity and $(\mathcal{S}_p^h)_n$ for pressure, and the corresponding test function spaces $(\mathcal{V}_{\mathbf{u}}^h)_n$ and $(\mathcal{V}_p^h)_n$ are defined as follows:

$$\left(\mathcal{S}_{\mathbf{u}}^h\right)_n = \left\{\mathbf{u}^h \,|\, \mathbf{u}^h \in [H^{1h}(Q_n)]^{n_{sd}}, \mathbf{u}^h \doteq \mathbf{g}^h \text{ on } (P_n)_g\right\}, \tag{12}$$

$$\left(\mathcal{V}_{\mathbf{u}}^h\right)_n = \left\{\mathbf{w}^h \,|\, \mathbf{w}^h \in [H^{1h}(Q_n)]^{n_{sd}}, \mathbf{w}^h \doteq \mathbf{0} \text{ on } (P_n)_g\right\}, \tag{13}$$

$$\left(\mathcal{S}_p^h\right)_n = \left(\mathcal{V}_p^h\right)_n = \left\{q^h \,|\, q^h \in H^{1h}(Q_n)\right\}. \tag{14}$$

Here $H^{1h}(Q_n)$ is the finite-dimensional function space over the space–time slab Q_n. Over the element domain, this space is formed by using first-order polynomials in both space and time. The interpolation functions are continuous in space but discontinuous in time.

The stabilized finite element formulation is written as follows: Given $(\mathbf{u}^h)_n^-$, find $\mathbf{u}^h \in (\mathcal{S}_{\mathbf{u}}^h)_n$ and $p^h \in (\mathcal{S}_p^h)_n$ such that $\forall \mathbf{w}^h \in (\mathcal{V}_{\mathbf{u}}^h)_n$ and $q^h \in (\mathcal{V}_p^h)_n$,

$$\int_{Q_n} \mathbf{w}^h \cdot \rho\left(\frac{\partial \mathbf{u}^h}{\partial t} + \mathbf{u}^h \cdot \nabla \mathbf{u}^h - \mathbf{f}^h\right) \mathrm{d}Q + \int_{Q_n} \boldsymbol{\varepsilon}(\mathbf{w}^h) : \boldsymbol{\sigma}(p^h, \mathbf{u}^h)\, \mathrm{d}Q - \int_{(P_n)_h} \mathbf{w}^h \cdot \mathbf{h}^h\, \mathrm{d}P + \int_{Q_n} q^h \nabla \cdot \mathbf{u}^h\, \mathrm{d}Q$$
$$+ \int_{\Omega_n} (\mathbf{w}^h)_n^+ \cdot \rho\left((\mathbf{u}^h)_n^+ - (\mathbf{u}^h)_n^-\right) \mathrm{d}\Omega + \sum_{e=1}^{(n_{\mathrm{el}})_n} \int_{Q_n^e} \frac{\tau_{\mathrm{LSME}}}{\rho}\left[\rho\left(\frac{\partial \mathbf{w}^h}{\partial t} + \mathbf{u}^h \cdot \nabla \mathbf{w}^h\right) - \nabla \cdot \boldsymbol{\sigma}(q^h, \mathbf{w}^h)\right]$$
$$\cdot\left[\rho\left(\frac{\partial \mathbf{u}^h}{\partial t} + \mathbf{u}^h \cdot \nabla \mathbf{u}^h\right) - \nabla \cdot \boldsymbol{\sigma}(p^h, \mathbf{u}^h) - \rho \mathbf{f}^h\right] \mathrm{d}Q + \sum_{e=1}^{n_{\mathrm{el}}} \int_{Q_n^e} \tau_{\mathrm{LSIC}} \nabla \cdot \mathbf{w}^h \rho \nabla \cdot \mathbf{u}^h\, \mathrm{d}Q = 0. \tag{15}$$

This formulation is sequentially applied to all of the space–time slabs $Q_0, Q_1, Q_2, \ldots, Q_{N-1}$. The computation starts with

$$(\mathbf{u}^h)_0^- = \mathbf{u}_0, \qquad \nabla \cdot \mathbf{u}_0 = 0 \quad \text{on } \Omega_0. \tag{16}$$

Here τ_{LSME} and τ_{LSIC} are the stabilization parameters (see [1,20]). For an earlier detailed reference on this stabilized formulation, see [6].

4. Finite element formulation for structural mechanics

Consider Ω^s as the spatial structural mechanics domain where the subscript t has been dropped to simplify the notation. The domain Ω^s is discretized into subdomains $(\Omega^s)^e$, $e = 1, 2, \ldots, n_{\mathrm{el}}^s$, where n_{el}^s is the number of structural mechanics elements. For this discretization, the finite element trial function space $\mathscr{S}^h$ for displacement, and the corresponding test function space $\mathscr{V}^h$ are defined as follows:

$$\mathscr{S}^h = \left\{\mathbf{y}^h \,|\, \mathbf{y}^h \in [H^{1h}(\Omega^s)]^{n_{xd}},\ \mathbf{y}^h \doteq (\mathbf{g}^s)^h \text{ on } \Gamma_g^s\right\}, \tag{17}$$

$$\mathscr{V}^h = \left\{\delta\mathbf{y}^h \,|\, \delta\mathbf{y}^h \in [H^{1h}(\Omega^s)]^{n_{xd}},\ \delta\mathbf{y}^h \doteq \mathbf{0} \text{ on } \Gamma_g^s\right\}. \tag{18}$$

Here $H^{1h}(\Omega^s)$ is the finite-dimensional function space over Ω^s. Applying the principle of virtual work, the finite element formulation is written as follows: Find $\mathbf{y}^h \in \mathscr{S}^h$ such that $\forall \delta\mathbf{y}^h \in \mathscr{V}^h$,

$$\int_{\Omega^s} \rho^s \frac{\mathrm{d}^2 \mathbf{y}^h}{\mathrm{d}t^2} \cdot \delta\mathbf{y}^h\, \mathrm{d}\Omega^s + \int_{\Omega^s} \mathbf{S}^h : \delta\mathbf{E}^h\, \mathrm{d}\Omega^s = \int_{\Gamma_h^s} (\mathbf{h}^s)^h \cdot \delta\mathbf{y}^h\, \mathrm{d}\Gamma^s + \int_{\Omega^s} \rho^s \mathbf{f}^h \cdot \delta\mathbf{y}^h\, \mathrm{d}\Omega^s. \tag{19}$$

5. Numerical example

The flow conditions used here are the same as those used in [5], where we computed with the MDM the aerodynamics of a rigid parachute crossing an aircraft wake.

The aircraft is assumed to be traveling at 200 ft/s, with an angle of attack of 10 degrees. The Reynolds number based on the aircraft length and flight speed is set to 2×10^9, which is about nine times larger than the typical value corresponding to the expected flight conditions. In non-dimensional numbers, the aircraft length is taken as 8.8 units, and the flight speed as 1 unit. The long-wake flow computed in [5] is used here to define the flow conditions the parachute is subjected to as it traverses the space also covered by the wake domain. This wake flow was computed in a coordinate frame attached to the aircraft, and we take this into account when we extract from the wake flow data the boundary conditions we use in computation of the parachute fluid–structure interactions. We assume that the two aircraft are flying at the same speed. We also assume that at the end of a short, initial period following the deployment of the parachute, its horizontal velocity becomes zero relative to the ground, and it attains a descent velocity of 20 ft/s. In this paper, we focus on this second phase of the parachute trajectory, which can be represented by an oblique line with a tangent of 0.1. For this study, we select approximately the midpoint between the wingtip and the outer engine as the lateral position relative to the aircraft that the parachute crosses the wake.

The parachute is modeled after a US Army C-9 personnel parachute, with 28 suspension lines. These lines extend through the canopy as reinforcements. We include a barrel-shaped payload in our model. This payload is positioned relative to the parachute in such a way that the suspension lines join at the top of the payload.

The structural model for the parachute starts with a canopy that is flat and of circular shape. The finite element mesh for the parachute structure is made of 4509 nodes, 8288 triangular membrane elements, and 1120 two-noded cable elements (see the left picture in Fig. 1). First a stand-alone structural mechanics computation is carried out to inflate the canopy with a uniform pressure differential prescribed on the canopy surface. After this inflation, the canopy diameter becomes approximately 1.2 (see the right picture in Fig. 1). This inflated shape is used in defining the initial conditions for the structure in computation of the fluid–structure interactions.

The dimensions of the parachute domain are 9.5 in height and 7×7 in the horizontal plane. The Reynolds number based on the parachute diameter and the descent velocity of 20 ft/s is 2.33×10^6.

Using the triangular mesh for the canopy as an interior surface mesh, a volume mesh in generated for the fluid domain. This mesh is made of 212,177 nodes, 1,286,063 tetrahedral elements in the interior, and 10,089 prismatic elements in the one-element-thick layer surrounding the domain (see Fig. 2).

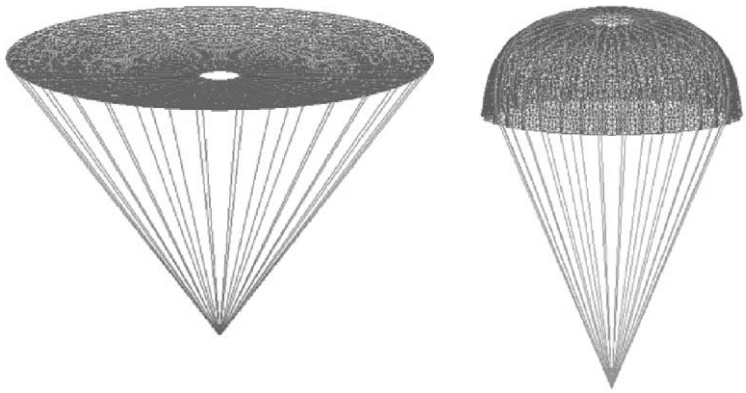

Fig. 1. Mesh for the parachute structure. Initial (left) and inflated (right) geometries.

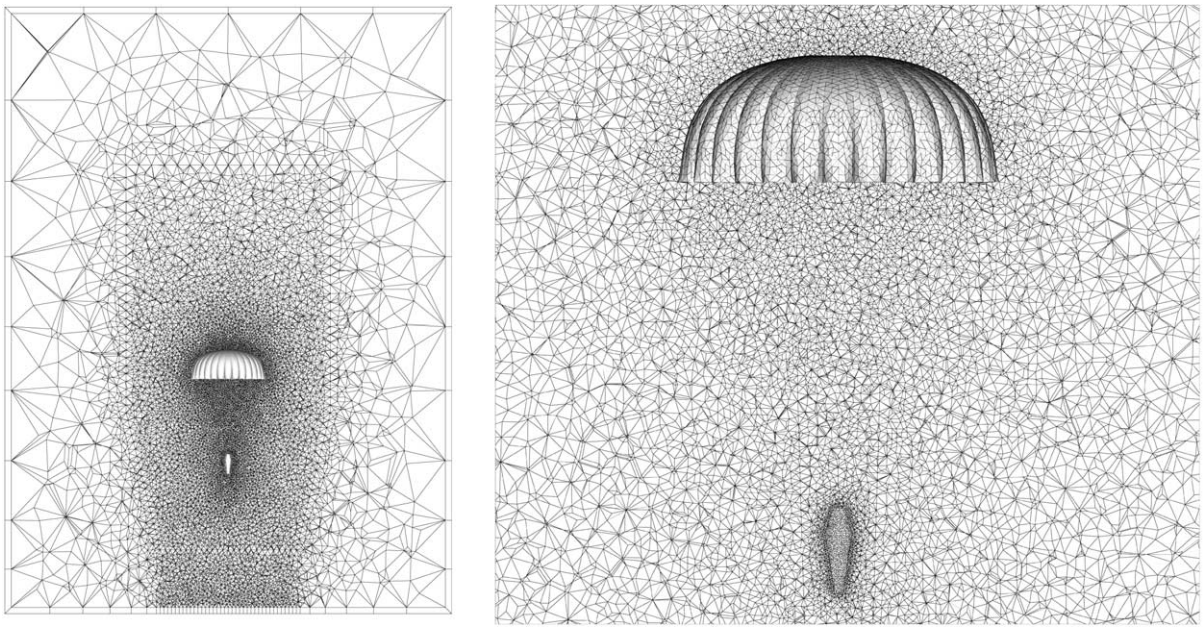

Fig. 2. Initial mesh for the parachute domain.

The boundary conditions for the fluid dynamics part of the problem consist of inflow conditions at the bottom and side boundaries, outflow conditions at the top boundary, and no-slip on the parachute and payload surfaces. The velocity conditions at the inflow and the stress conditions at the outflow are extracted from the wake flow data computed in [5]. The extracted velocity boundary conditions are modified to take into account the parachute trajectory. In describing the results here, $t = 0$ marks the beginning of the second phase of the trajectory that we are focusing on. In this computation the time step size is 0.005.

Fig. 3 shows the vertical component of the velocity for a parachute descending through a wake-free air (i.e., the parachute is in a uniform vertical flow) and the parachute crossing the wake. These results

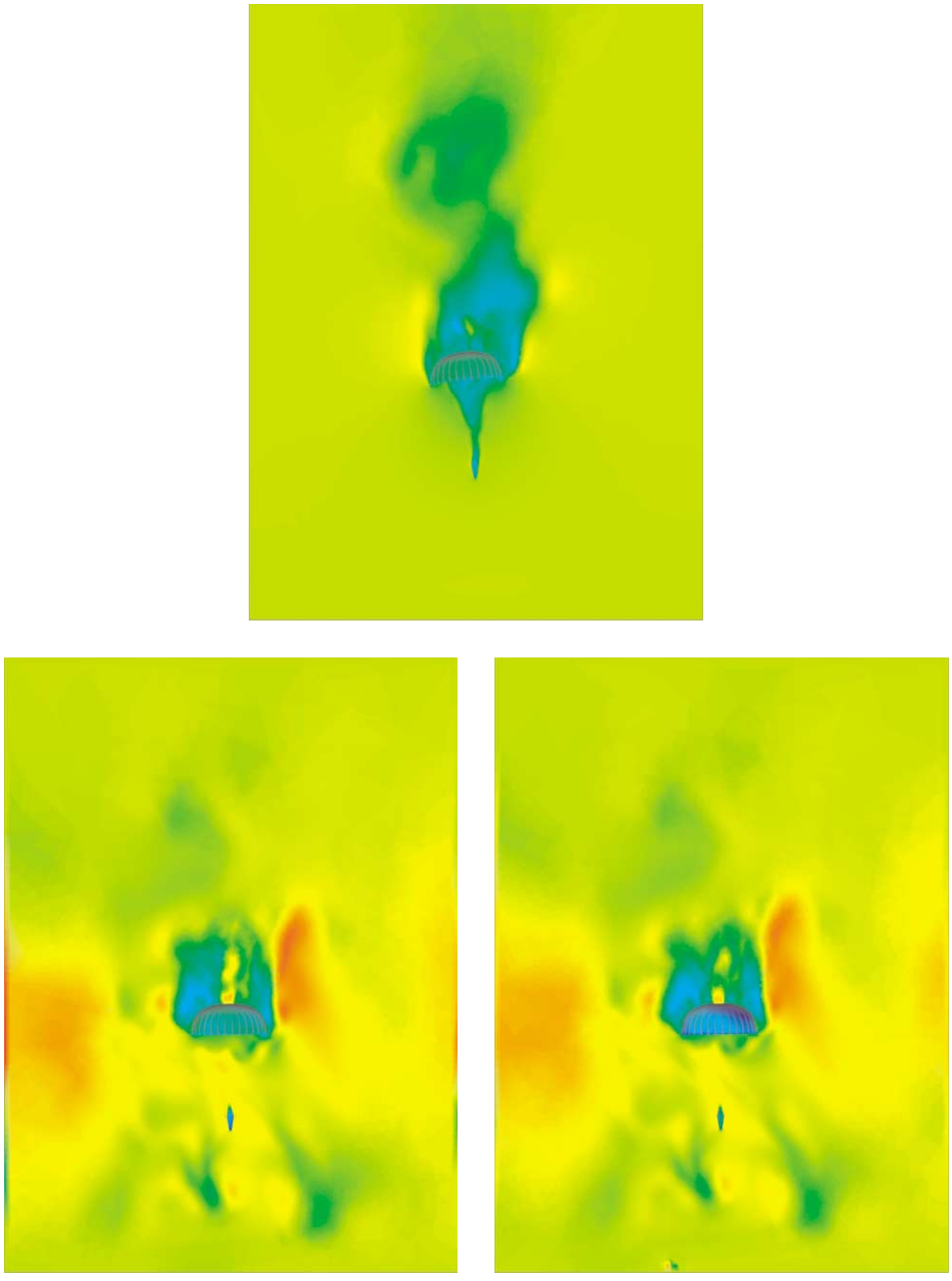

Fig. 3. Vertical component of the velocity in the centered vertical plane, and the pressure distribution on the parachute and payload surfaces. Parachute in uniform flow (upper), and in the wake at $t = 0.49$ (lower left) and $t = 0.62$ (lower right).

correspond to the centered vertical plane, and are displayed at two different instants for the parachute in the wake. Fig. 4 shows the pressure distribution on the upper and lower surfaces of the parachute for the one in uniform flow and the one crossing the wake. The pressure values for the parachute crossing the wake are displayed at the same time steps as those in Fig. 3. We note that the pressure on the lower surface is always higher than it is on the upper surface. Fig. 5 shows the aerodynamical forces acting on the parachute for the one in uniform flow and the one in the wake. Fig. 6 shows the distribution of the maximum principal stress for the canopy. The stresses for the parachute crossing the wake are displayed at the same time steps as those in Fig. 3. We note the non-symmetric deformation of the parachute canopy at these time steps.

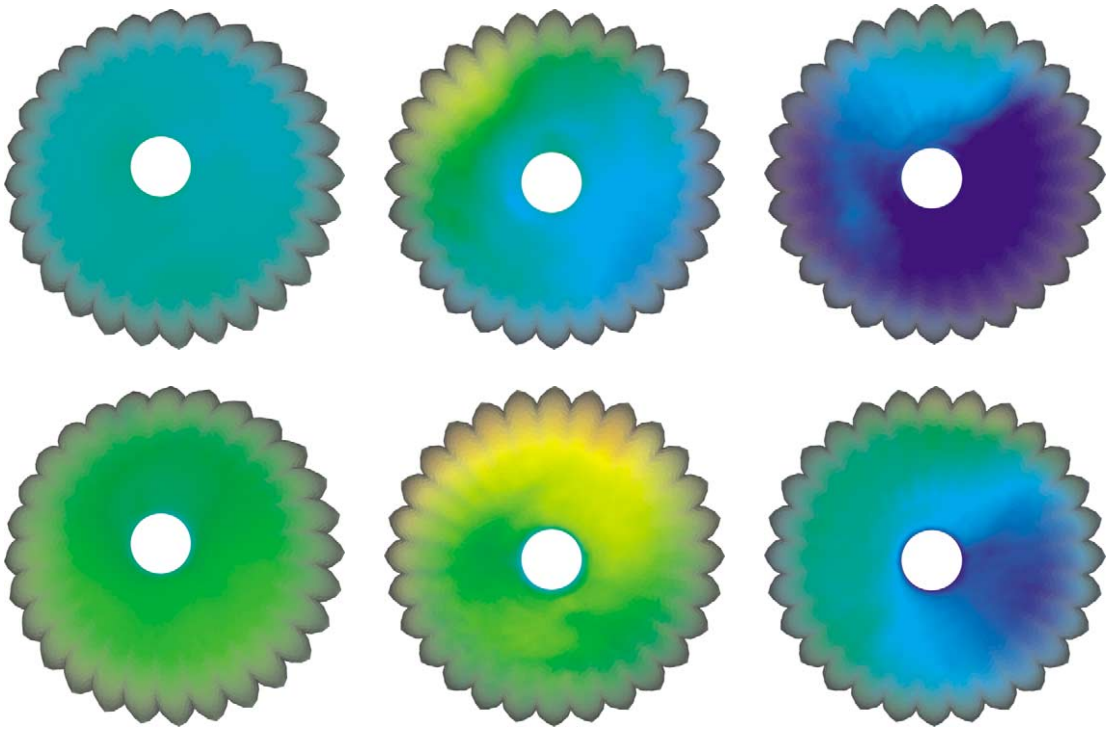

Fig. 4. Pressure distribution on the parachute surface. Parachute in uniform flow (left), and in the wake at $t = 0.49$ (middle) and $t = 0.62$ (right). The upper and lower parachute surfaces are shown, respectively, in the upper and lower rows of pictures.

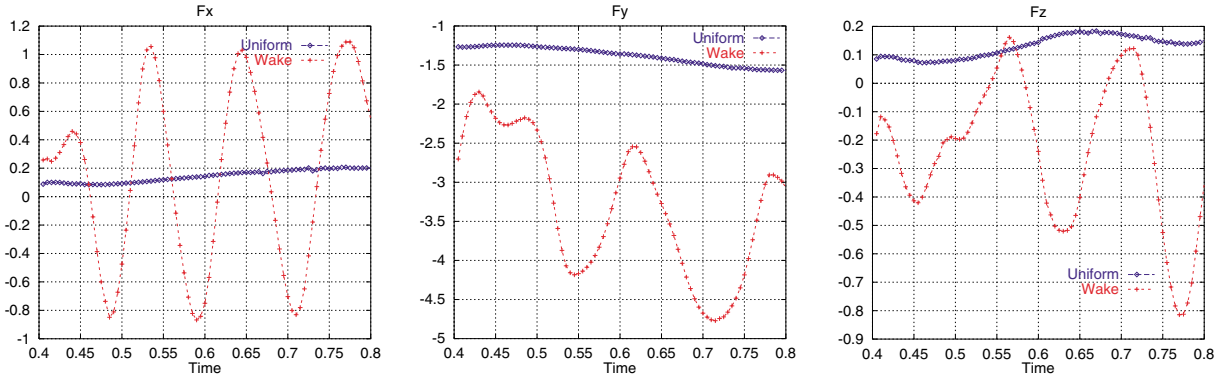

Fig. 5. Time history of the aerodynamical forces acting on the parachute for the one in uniform flow and the one in the wake. Graphs show the forces in the aircraft's flight direction (left), the vertical drag (middle), and the force in lateral direction (right).

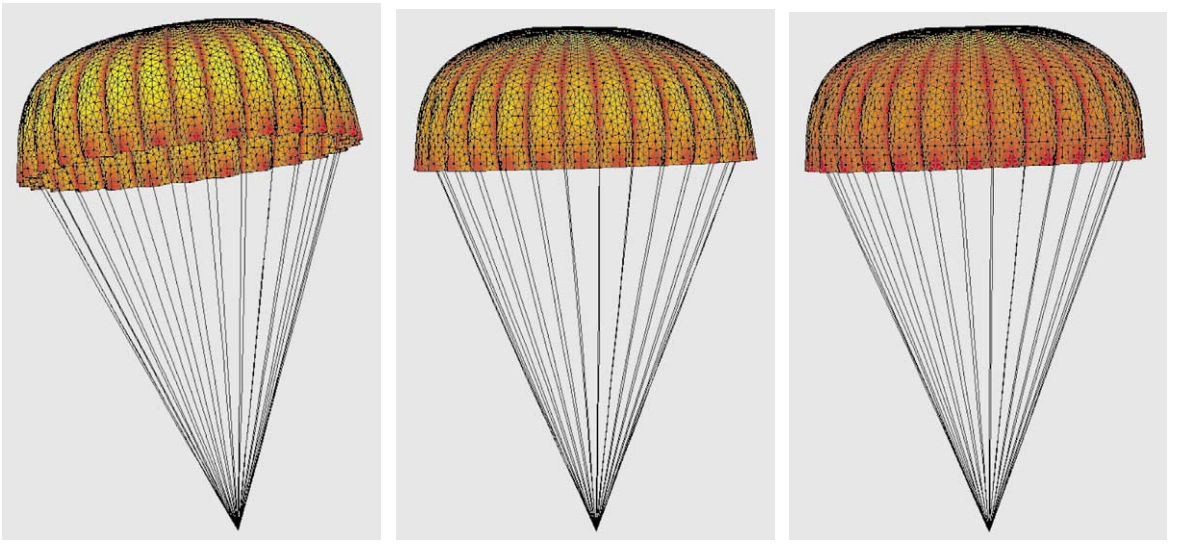

Fig. 6. Maximum principal stress for the parachute canopy. Parachute in uniform flow (left), and in the wake at $t = 0.49$ (middle) and $t = 0.62$ (right).

6. Concluding remarks

We described a computational technique designed for simulation of the fluid–structure interactions of a parachute crossing the far wake of an aircraft. In this technique, the flow conditions the parachute is subjected to are extracted from the long-wake flow data already computed. In general, the wake flow data may have been computed earlier for some other related purpose, or may have been computed specifically for the parachute problem we wish to simulate. In our case, the wake flow data were computed earlier, with the MDM, for the purpose of simulating the aerodynamics of a rigid parachute crossing the aircraft wake.

The parachute was first inflated with a uniform pressure to a shape to be used as initial condition for the structure in computation of the fluid–structure interactions. Then, the parachute is placed in a domain that moves with the payload and traverses the space also covered by the wake flow domain. The boundary conditions for the parachute computations are extracted as inflow velocity and outflow stress conditions from the wake flow domain, at locations corresponding to the positions of the boundaries of the parachute domain.

The DSD/SST formulation was used for solving the Navier–Stokes equations of incompressible flows. This method automatically takes into account the motion of the boundaries and interfaces. A mesh moving technique was used in conjunction with the DSD/SST formulation to update the mesh every time step. The finite element formulation used for solving the structural mechanics equations for the parachute canopy and suspension lines is coupled to the DSD/SST formulation.

With the numerical example we included in this paper, we were able to show that the computational technique described here can be used as a special-purpose module of the MDM developed for the class of problems considered here, and that the resulting computational method can be used to address the challenges inherent in the simulation of the fluid–structure interactions of a parachute crossing an aircraft wake.

Acknowledgements

This work was supported by NASA Johnson Space Center (grant no. NAG9-1059), AFOSR (contract no. F49620-98-1-0214), and by the US Army Natick Soldier Center (contract no. DAAD16-00-C-9222). The content does not necessarily reflect the position or the policy of the government, and no official endorsement should be inferred. The second author was supported by the Bridgestone Corp.

References

[1] T.E. Tezduyar, Y. Osawa, Methods for parallel computation of complex flow problems, Parallel Computing 25 (1999) 2039–2066.
[2] Y. Osawa, V. Kalro, T.E. Tezduyar, Multi-domain parallel computation of wake flows, Computer Methods in Applied Mechanics and Engineering 174 (1999) 371–391.
[3] Y. Osawa, T.E. Tezduyar, A multi-domain method for 3D computation of wake flow behind a circular cylinder, Computational Fluid Dynamics Journal 8 (1999) 296–308.
[4] Y. Osawa, T.E. Tezduyar, 3D simulation and visualization of unsteady wake flow behind a cylinder, Journal of Visualization 2 (1999) 127–134.
[5] T.E. Tezduyar, Y. Osawa, The multi-domain method for computation of the aerodynamics of a parachute crossing the far wake of an aircraft, Computer Methods in Applied Mechanics and Engineering 191 (2001) 705–716, this issue.
[6] T.E. Tezduyar, Stabilized finite element formulations for incompressible flow computations, Advances in Applied Mechanics 28 (1991) 1–44. ⟵ (1992)
[7] T.E. Tezduyar, M. Behr, J. Liou, A new strategy for finite element computations involving moving boundaries and interfaces – the deforming-spatial-domain/space–time procedure: I. The concept and the preliminary tests, Computer Methods in Applied Mechanics and Engineering 94 (1992) 339–351.
[8] T.E. Tezduyar, M. Behr, S. Mittal, J. Liou, A new strategy for finite element computations involving moving boundaries and interfaces – the deforming-spatial-domain/space–time procedure: II. Computation of free-surface flows, two-liquid flows, and flows with drifting cylinders, Computer Methods in Applied Mechanics and Engineering 94 (1992) 353–371.
[9] T.J.R. Hughes, G.M. Hulbert, Space–time finite element methods for elastodynamics: formulations and error estimates, Computer Methods in Applied Mechanics and Engineering 66 (1988) 339–363.
[10] T.J.R. Hughes, L.P. Franca, G.M. Hulbert, A new finite element formulation for computational fluid dynamics: VIII. the Galerkin/least-squares method for advective–diffusive equations, Computer Methods in Applied Mechanics and Engineering 73 (1989) 173–189.
[11] P. Hansbo, A. Szepessy, A velocity–pressure streamline diffusion finite element method for the incompressible Navier–Stokes equations, Computer Methods in Applied Mechanics and Engineering 84 (1990) 175–192.
[12] T.J.R. Hughes, A.N. Brooks, A multi-dimensional upwind scheme with no crosswind diffusion, in: T.J.R. Hughes (Ed.), Finite Element Methods for Convection Dominated Flows, AMD, vol. 34, ASME, New York, 1979, pp. 19–35.
[13] A.N. Brooks, T.J.R. Hughes, Streamline upwind/Petrov–Galerkin formulations for convection dominated flows with particular emphasis on the incompressible Navier–Stokes equations, Computer Methods in Applied Mechanics and Engineering 32 (1982) 199–259.
[14] T.E. Tezduyar, M. Behr, S. Mittal, A.A. Johnson, Computation of unsteady incompressible flows with the finite element methods – space–time formulations, iterative strategies and massively parallel implementations, in: P. Smolinski, W.K. Liu, G. Hulbert, K. Tamma (Eds.), New Methods in Transient Analysis, AMD, vol. 143, ASME, New York, 1992, pp. 7–24.
[15] K. Stein, R. Benny, V. Kalro, T.E. Tezduyar, J. Leonard, M. Accorsi, Parachute fluid–structure interactions: 3-D Computation, Computer Methods in Applied Mechanics and Engineering 190 (2000) 373–386.
[16] V. Kalro, T. Tezduyar, A parallel 3D computational method for fluid–structure interactions in parachute systems, Computer Methods in Applied Mechanics and Engineering 190 (2000) 321–332.
[17] Y. Saad, M. Schultz, GMRES: a generalized minimal residual algorithm for solving nonsymmetric linear systems, SIAM Journal of Scientific and Statistical Computing 7 (1986) 856–869.
[18] K.J. Bathe, Finite Element Procedures, Prentice-Hall, Englewood Cliffs, NJ, 1996.
[19] A. Lo, Nonlinear dynamic analysis of cable and membrane structure, Ph.D. Thesis, Department of Civil Engineering, Oregon State University, 1982.
[20] M. Behr, T.E. Tezduyar, Finite element solution strategies for large-scale flow simulations, Computer Methods in Applied Mechanics and Engineering 112 (1994) 3–24.